Proc. Natl. Acad. Sci. USA
Vol. 92, pp. 10252–10256, October 1995
Cell Biology

Contraction due to microtubule disruption is associated with increased phosphorylation of myosin regulatory light chain

MICHAEL S. KOLODNEY AND ELLIOT L. ELSON

Department of Biochemistry and Molecular Biophysics, Washington University School of Medicine, St. Louis, MO 63110

Communicated by Carl Frieden, Washington University School of Medicine, St. Louis, MO, July 3, 1995 (received for review February 2, 1994)

ABSTRACT **Microtubules have been proposed to function as rigid struts which oppose cellular contraction. Consistent with this hypothesis, microtubule disruption strengthens the contractile force exerted by many cell types. We have investigated an alternative explanation for the mechanical effects of microtubule disruption: that microtubules modulate the mechanochemical activity of myosin by influencing phosphorylation of the myosin regulatory light chain (LC_{20}). We measured the force produced by a population of fibroblasts within a collagen lattice attached to an isometric force transducer. Treatment of cells with nocodazole, an inhibitor of microtubule polymerization, stimulated an isometric contraction that reached its peak level within 30 min and was typically 30–45% of the force increase following maximal stimulation with 30% fetal bovine serum. The contraction following nocodazole treatment was associated with a 2- to 4-fold increase in LC_{20} phosphorylation. The increases in both force and LC_{20} phosphorylation, after addition of nocodazole, could be blocked or reversed by stabilizing the microtubules with paclitaxel (former generic name, taxol). Increasing force and LC_{20} phosphorylation by pretreatment with fetal bovine serum decreased the subsequent additional contraction upon microtubule disruption, a finding that appears inconsistent with a load-shifting mechanism. Our results suggest that phosphorylation of LC_{20} is a common mechanism for the contractions stimulated both by microtubule poisons and receptor-mediated agonists. The modulation of myosin activity by alterations in microtubule assembly may coordinate the physiological functions of these cytoskeletal components.**

Microtubule disruption induces a contraction in a strikingly diverse variety of tissue culture cells (1–4). The "force counterbalance" or "tensegrity" model of cytoskeletal structure explains this contraction as a transfer of contractile load from internal struts (microtubules) to sites of extracellular anchorage (5, 6). The tensegrity model provides a simple and elegant explanation for the mechanical effects of microtubule inhibitors that is consistent with many experimental observations. Nevertheless, measurements of the micromechanical loads upon specific cytoskeletal components of intact cells have not yet been achieved (7), and so direct experimental verification of this model is not presently possible.

An obvious alternative to the tensegrity model, that microtubule disruption increases tension through activation of cellular contractile elements, has received less attention. Microtubules or microtubule-associated proteins may influence the dynamic properties of the actin cytoskeleton. Microtubule depolymerization can block or reverse the disruption of actin stress fibers by phorbol ester (1, 8). Proteins have been identified that bind to both microtubules and actin filaments (9–12). It has been suggested (1) that depolymerization of microtubules may release associated proteins that organize actin filaments (12, 13), possibly resulting in increased tension.

Microtubules may directly interact with intracellular signaling pathways. For example, disruption of microtubules can enhance transduction of signals mediated by GTP-binding proteins (14) or activate cellular protein kinases (15). In addition, some protein kinases physically associate with microtubules (16–18). Thus, microtubule disruption might initiate biochemical signals which activate the force-generating components of the cytoskeleton. This activation could be sufficient to account for both increased tension (19) and changes in actin organization (20).

The major force-generating system of fibroblasts is composed of a cytoplasmic network of actin and myosin. Nonmuscle cells regulate actin–myosin interactions through reversible phosphorylation of the myosin regulatory light chain (LC_{20}) (19, 21–25), a mechanism analogous to the regulation of smooth muscle contraction. Thus, we can test the hypothesis that the mechanical consequences of microtubule disruption are mediated through activation of cytoplasmic myosin motor activity by correlating LC_{20} phosphorylation levels with isometric force.

We have previously described a technique designed to measure the tension exerted by fibroblasts cultured in a collagen matrix (19, 26) and have used this approach to demonstrate that microtubule disruption results in a 2- to 3-fold increase in force. This contraction is of similar magnitude to that following stimulation with thrombin, a mitogen known to produce large intracellular free Ca^{2+} transients (26). We subsequently established a correlation between isometric tension and LC_{20} phosphorylation in thrombin-stimulated chick embryo fibroblasts (CEFs) analogous to that documented in smooth muscle (19).

In this report, we explore the possibility that microtubules regulate contraction by controlling the mechanochemical activity of myosin through phosphorylation of LC_{20}. In addition, we quantitatively study the interactions between contraction stimulated by microtubule disruption and contraction stimulated through receptor-mediated agonists.

MATERIALS AND METHODS

Cell Culture. CEFs (a generous gift of Milton Schlesinger, Washington University) isolated from 11-day chicken embryos were maintained in Dulbecco's modified Eagle's medium (DMEM) supplemented with 10% fetal bovine serum (FBS), penicillin at 50 units/ml, and streptomycin at 50 μg/ml. Primary cultures were passaged 4 days after isolation and were used to make fibroblast-populated collagen gel samples or plated on 35-mm tissue culture dishes for phosphorylation measurements 1–2 days following this first passage.

Isometric Tension Apparatus. Isometric tension was measured by a published technique (19), with modifications. Strips of Velcro were glued to 1.4-cm glass rods (2.5-mm outer diameter) with "self-leveling" Silastic adhesive (Dow Corn-

The publication costs of this article were defrayed in part by page charge payment. This article must therefore be hereby marked "*advertisement*" in accordance with 18 U.S.C. §1734 solely to indicate this fact.

Abbreviations: CEF, chicken embryo fibroblast; FBS, fetal bovine serum; FPCL, fibroblast-populated collagen lattice; LC_{20}, regulatory light chain.

ing). The rods were separated by spacers and placed in rectangular wells (1.5 cm × 1.6 cm). Nine hundred eighty microliters of ice-cold DMEM/10% FBS containing CEFs at 0.9×10^6 cells per ml and rat tail collagen (Upstate Biotechnology, Lake Placid, NY) at 1.0–1.2 mg/ml was poured between the rods. The medium bathing the cells was replaced with serum-free DMEM 24 hr after the gels were cast.

After 24–48 hr in serum-free medium, the preparation was mounted on the force transducer (19) and then restretched to its original length. After 30–60 min, baseline force reached a steady value, and agonists were added. In some experiments the tissue partially detached from the Velcro under the increased tension from FBS stimulation. Experiments in which >10% of the samples detached were eliminated from the final data analysis.

Measurement of Light-Chain Phosphorylation. Phosphorylation measurements were performed on CEFs in collagen lattice "discs" adherent to 35-mm tissue culture dishes or on monolayer cultures prepared by seeding 4×10^5 CEFs per 35-mm tissue culture dish as indicated in the figure captions. Cell-populated collagen discs were prepared by placing a 300-μl drop of DMEM containing cells at 1.2×10^6 per ml and collagen at 0.75 mg/ml in the center of a dry 35-mm tissue culture dish, similar to the method of Tomasek *et al.* (27). The collagen solution was warmed to room temperature for 30 sec prior to placement of the drop on the tissue culture dish.

For phosphorylation measurements, cells were precipitated in ice-cold 10% trichloroacetic acid/2 mM dithiothreitol. Precipitate scraped from dishes or from cell-populated collagen lattices was washed once with 1 ml of acetone/2 mM dithiothreitol and dried on ice. Pellets were solubilized in 80 μl of 9.0 M urea/2 mM dithiothreitol/20 mM Tris/22 mM glycine/1 mM EGTA/250 mM sucrose at pH 8.8 with the aid of a bath sonicator.

Glycerol/urea/PAGE with immunoblotting was carried out by a modification of the procedure of Taylor and Stull (28) as described (19) or, in later experiments, the signal was enhanced with the following modifications. Protein was transferred to nitrocellulose in 23 mM glycine/20 mM Tris, pH 8.8/20% methanol. After transfer, the nitrocellulose membrane was incubated with 1% glutaraldehyde in phosphate-buffered saline for 5 min, washed three times in phosphate-buffered saline, and rinsed twice for 1 min with 0.1% $NaBH_4$. The membrane with then blocked overnight at room temperature with 5% nonfat dry milk. LC_{20} was detected with a 1:1000 dilution of an affinity-purified rabbit antibody (a gift of Primal de Lannerole, University of Illinois) followed by ECL reagents (Amersham).

RESULTS

Contractility Is Coupled to Microtubule Disruption and Assembly. We measured the increase in the contractile force exerted by CEFs in fibroblast-populated collagen lattices (FPCLs) upon disruption of microtubules. Contraction was often apparent within seconds after addition of nocodazole (Fig. 1*A*). Force typically increased 1–2 mN before reaching a steady level within about 30 min.

Treatment of cells with paclitaxel (former generic name, taxol) stabilizes microtubules to subsequent disruption by nocodazole (1, 29). Pretreatment of CEFs with paclitaxel, 20 min prior to the addition of nocodazole, stabilizes microtubules to disruption (demonstrated by immunofluorescence, data not shown). Thus, paclitaxel-treated cells provide a control for any side effects of nocodazole which do not result from microtubule disruption.

Paclitaxel (10 μM) entirely inhibited the nocodazole-induced contraction (Fig. 1 *B* and *C*). The ability of paclitaxel to block contraction was specific for microtubule-disrupting

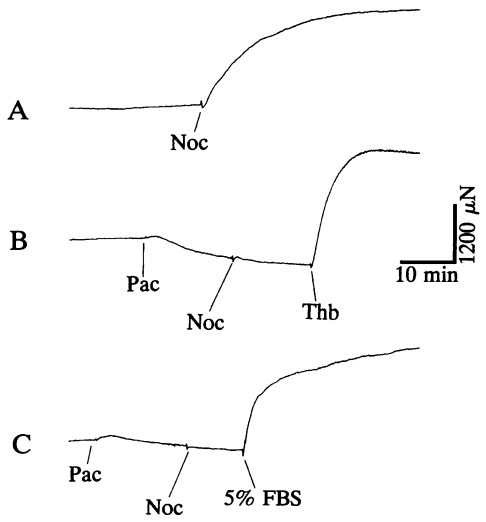

FIG. 1. Specific block of nocodazole contraction by paclitaxel. FPCLs were mounted on force transducers (see *Materials and Methods*). Results are representative of at least three experiments. (*A*) Nocodazole (Noc, 5 μM) stimulated a contraction that typically reached maximal levels within about 30 min. (*B*) Addition of paclitaxel (Pac, 10 μM) usually resulted in a small relaxation. Paclitaxel pretreatment (20 min) completely inhibited the nocodazole contraction but had little effect on contraction stimulated by a saturating dose of thrombin (Thb, 1 unit/ml). (*C*) Paclitaxel (10 μM) pretreatment had little effect on contraction stimulated by 5% FBS.

agents, since contractions stimulated by thrombin (Fig. 1*B*) or 5% FBS (Fig. 1*C*) were not blocked in paclitaxel-treated cells.

Paclitaxel Reverses the Nocodazole-Induced Contraction. Because paclitaxel reverses microtubule disruption in nocodazole-treated cells, even in the continued presence of nocodazole (29), we tested the mechanical effect of adding paclitaxel to cells precontracted with nocodazole. Paclitaxel (in the continuous presence of nocodazole) stimulated a strikingly rapid relaxation (Fig. 2*A*). Force was reduced to its pre-nocodazole level within 5 min of paclitaxel addition and then typically declined an additional 200–300 μN at a slower rate. Cells relaxed in this manner still retained the ability to contract in response to thrombin (Fig. 2*A*). The rapid relaxation after paclitaxel was specific for nocodazole-contracted cells, since paclitaxel showed little effect on cells contracted with thrombin or FBS (Fig. 2 *B* and *C*).

Time Course of Nocodazole- and FBS-Stimulated Contractions. Force increased rapidly in the first few minutes following addition of FBS and continued to increase at a slower rate throughout the entire 2-hr monitoring period (Fig. 3). The contraction in response to nocodazole reached a maximum at about 30 min before declining slowly to 80% of its maximal value at 2 hr (Fig. 3).

Microtubule Disruption Is Associated with Increased LC_{20} Phosphorylation. By measuring changes in LC_{20} phosphorylation following the addition of nocodazole, we investigated the possibility that microtubule disruption causes contraction through myosin activation. We found relatively large variations in baseline LC_{20} phosphorylation between different preparations of CEFs. Nevertheless, LC_{20} phosphorylation levels both before and after stimulation with nocodazole, thrombin, or FBS were consistent among different samples from the same preparation of CEFs. In agreement with our previous findings (19), serum-starved CEFs typically had 10–40% of LC_{20} monophosphorylated with the remainder unphosphorylated. After nocodazole stimulation, monophosphorylated/diphosphorylated LC_{20} increased to 40–70%.

Addition of 5 μM nocodazole resulted in a LC_{20} phosphorylation increase which appeared nearly maximal by 30 min and

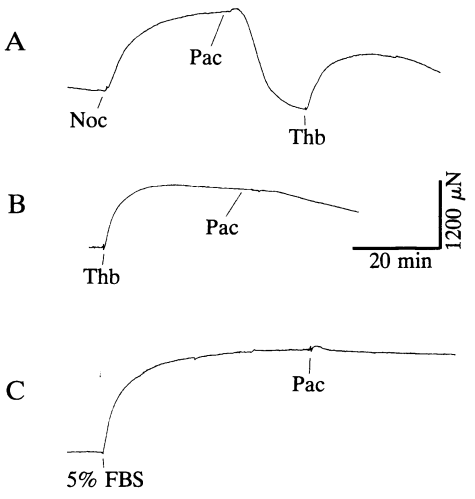

FIG. 2. Specific reversal of nocodazole contraction by paclitaxel. Results are representative of at least three experiments. (*A*) Addition of paclitaxel (Pac, 10 μM) rapidly reversed the nocodazole (Noc, 5 μM)-stimulated contraction (in the continued presence of nocodazole). Force was reduced to below pre-nocodazole levels within 5–10 min. Cells contracted and relaxed in this manner retained the capacity to contract in response to thrombin (Thb, 1 unit/ml). (*B* and *C*) Paclitaxel (10 μM) had little effect on cells contracted with thrombin (1 unit/ml) or 5% FBS.

which continued for at least 40 min after stimulation (Fig. 4). LC_{20} phosphorylation following nocodazole treatment was typically about equally divided between the mono- and diphosphorylated forms, although some experiments showed a significant preference toward the monophosphorylated form.

The LC_{20} phosphorylation after nocodazole was blocked by paclitaxel pretreatment or reversed by paclitaxel posttreatment (Fig. 5). Cells treated with 5 μM nocodazole for 20

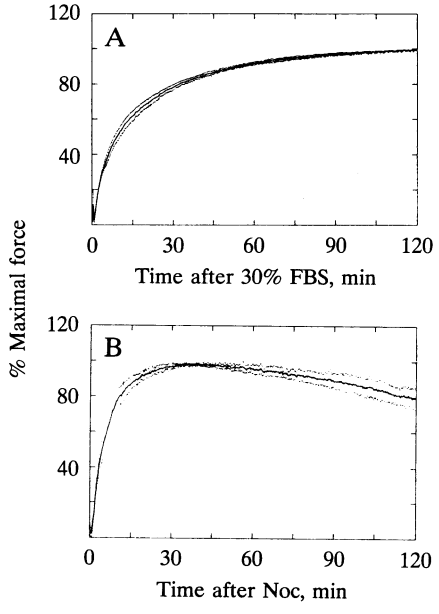

FIG. 3. Time course of contractions after FBS and nocodazole. Solid lines represent average response to FBS (*A*) or nocodazole (*B*) as a percentage of the maximal response to the particular agonist (n = 3). Dotted lines show standard error. CEFs stimulated with 30% FBS exhibited a rapid force increase in the first 5 min. Force continued to increase at a slower rate for the entire 2-hr period. The response to 10 μM nocodazole reached a maximum at about 30 min and then slowly declined.

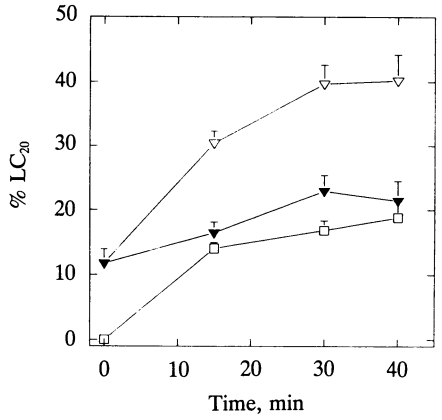

FIG. 4. Time course of LC_{20} phosphorylation increase after addition of nocodazole to CEFs within collagen lattice discs. Nocodazole (5 μM) was added at time 0. The percentage of LC_{20} monophosphorylated (▼) or diphosphorylated (□) and the sum of mono- and diphosphorylated LC_{20} (▽) are displayed. Error bars show standard error (n = 3). Results are representative of three similar experiments.

min followed by 10 μM paclitaxel for 20 min (without washout of nocodazole) or cells pretreated with 10 μM paclitaxel for 20 min before addition of 5 μM nocodazole for 20 min (without washout of paclitaxel) typically had LC_{20} phosphorylation levels below that of controls treated only with vehicle (dimethyl sulfoxide). This reduction in LC_{20} phosphorylation to below baseline levels was consistent with the corresponding force measurements (Fig. 1 *B* and *C* and Fig. 2*A*), which, following addition of paclitaxel, usually declined to below baseline levels as well.

Prestimulation with FBS Reduces the Nocodazole-Stimulated Contraction. To examine further a possible role for load shifting in the contraction due to microtubule disruption, we determined whether maximal precontraction of the cells by 30% FBS affected the strength of the nocodazole-induced contraction. FBS was used because it produced a relatively stable contraction, increasing only 4% between 80 and 120 min

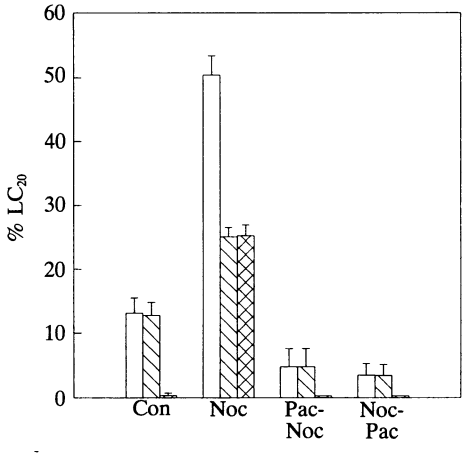

FIG. 5. Effect of microtubule stabilization by paclitaxel on the LC_{20} phosphorylation resulting from microtubule disruption. The percentage of total phosphorylated (sum of mono- and diphosphorylated) (open bars), monophosphorylated (hatched bars), and diphosphorylated (crosshatched bars) LC_{20} is displayed. Con, control cells treated with vehicle (dimethyl sulfoxide); Noc, 5 μM nocodazole for 20 min; Pac-Noc, 10 μM paclitaxel for 20 min followed by 5 μM nocodazole for 20 min (in the continued presence of paclitaxel); Noc-Pac, 5 μM nocodazole for 20 min followed by 10 μM paclitaxel for 20 min (in the continued presence of nocodazole). Error bars display standard error (n = 3).

(Fig. 3). Thus, the incremental effect of nocodazole was easiest to observe during this plateau in the FBS-stimulated contraction.

Force was measured over 110 min during which matched samples were treated either with 30% FBS for 80 min before addition of 10 μM nocodazole or with 10 μM nocodazole for 30 min before addition of 30% FBS. Total force was similar at the end of both protocols (Fig. 6). However, the response to nocodazole in cells precontracted with FBS was only 32% of the nocodazole response from cells not precontracted with FBS. The effect of FBS precontraction on the nocodazole response is actually underestimated in this experiment, since the FBS response contributes to some of the force rise after the addition of nocodazole (Fig. 3). Cells pretreated with nocodazole exhibited only 78% of the contractile response to FBS relative to cells with intact microtubules (Fig. 6).

We were concerned that the large stress of 30% FBS contraction might somehow cause mechanical damage to the preparation which could result in the reduced additional response to nocodazole. Therefore, we measured the contractile response to microtubule disruption in single preparations both before and after washout of FBS. In a representative example (Fig. 7), cells precontracted for 80 min with FBS generated an additional 780 μN after addition of nocodazole. However, after all agonists were washed out, a contraction of 1470 μN was measured in response to nocodazole. In four similar experiments, the nocodazole response after FBS was only 51 ± 5% of that after washout.

Increasing Phosphorylation with FBS Decreases the Additional Phosphorylation from Nocodazole. We sought to determine whether the decreased nocodazole-induced contraction of FBS-contracted cells was associated with a similarly blunted increase in LC_{20} phosphorylation. Cells showed a similar increase in LC_{20} phosphorylation after treatment with nocodazole (30 min) or FBS (80 or 120 min) (Fig. 8). The additional change in LC_{20} phosphorylation following microtubule disruption of FBS-contracted cells was small to insignificant. Thus, preactivation with FBS results in an even more blunted effect on the LC_{20} phosphorylation response to microtubule disruption than on the corresponding force change.

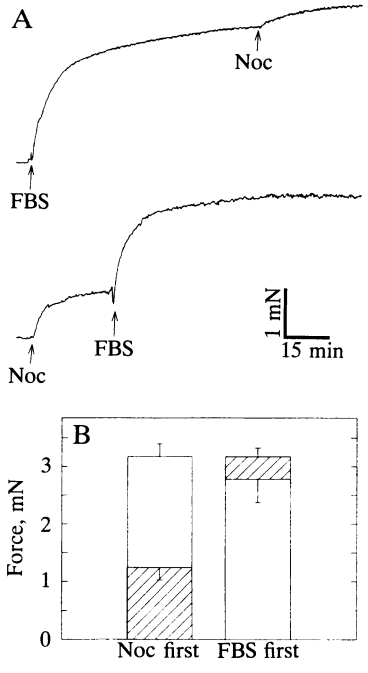

FIG. 6. Force response to a combination of FBS and nocodazole. (*A*) Cells were either contracted first with 30% FBS for 80 min before addition of 10 μM nocodazole (*Upper*) or contracted with 10 μM nocodazole for 30 min before addition of FBS (*Lower*). In both protocols force was monitored for 110 min following addition of the first stimulus. (*B*) A summary of three experiments performed as in *A*. The final force was similar whether FBS or nocodazole was added first. However, the incremental response to nocodazole (hatched bar) was reduced by a factor of ≈3 in FBS-activated cells.

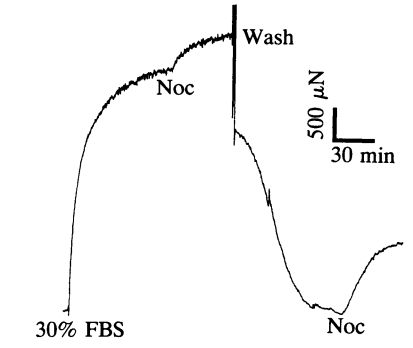

FIG. 7. Contractile response to nocodazole before and after washout of FBS. Cells were precontracted with 30% FBS. After 80 min in FBS, force reached a relatively steady level. At this time, microtubules were disrupted with 10 μM nocodazole (Noc) (without removal of the FBS). Force increased an additional 780 μN in the 40 min after nocodazole. However, following washout of FBS and nocodazole, cells produced about twice as large a contraction upon readdition of nocodazole. This figure is representative of four experiments.

DISCUSSION

Nocodazole Induces Contraction Through Microtubule Disruption. It appears highly unlikely that nocodazole stimulates contraction through a side effect rather than through microtubule disruption. Danowski (1) has shown that several microtubule inhibitors, all at very low concentrations, produce contractions of similar magnitude and that stabilization of microtubules with paclitaxel blocks the contractile activity of microtubule inhibitors. In Fig. 1, we demonstrate that paclitaxel pretreatment blocked the contractile effects of nocodazole but did not block contraction stimulated by FBS or thrombin. Therefore, paclitaxel blocked the nocodazole con-

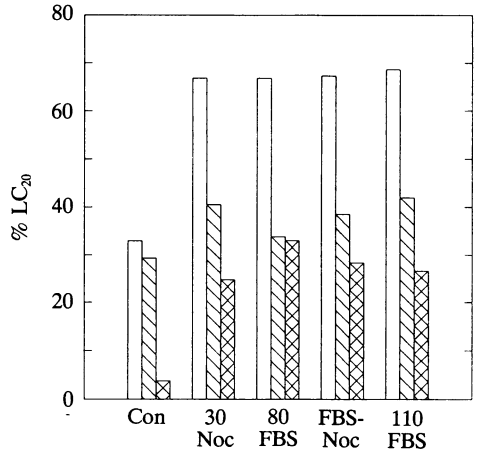

FIG. 8. LC_{20} phosphorylation after a combination of FBS and nocodazole. LC_{20} phosphorylation was measured in CEFs on 35-mm tissue culture dishes. The percentage of total phosphorylated (sum of mono- and diphosphorylated, open bars), monophosphorylated (hatched bars), and diphosphorylated (crosshatched bars) LC_{20} is displayed. CON, vehicle (dimethyl sulfoxide) for 120 min; Noc, 10 μM nocodazole for 30 min; 80 FBS, 30% FBS for 80 min; FBS-Noc, 30% FBS for 80 min after which 10 μM nocodazole was included for an additional 30 min without washout of FBS; 110 FBS, 30% FBS for 110 min.

traction specifically by stabilizing microtubules to nocodazole rather than by acting as a general inhibitor of contractility. The rapid reversal of contraction following repolymerization of microtubules by paclitaxel argues against a role for secretory products in mediating the nocodazole-stimulated contraction.

Mechanism of Contraction Resulting from Microtubule Disruption. The load-shifting and LC_{20} phosphorylation mechanisms predict opposite effects of preexisting myosin activation on nocodazole-stimulated contraction. If the force increase measured after nocodazole treatment was caused by contractile load shifting from microtubule struts to extracellular contacts, then increasing contractility by phosphorylating LC_{20} should increase the force that could be shifted off microtubules. If, however, the contraction resulting from microtubule disruption was due to LC_{20} phosphorylation, a prior contraction due to an increase in LC_{20} phosphorylation might saturate this response, resulting in a reduced additional contraction.

To determine the effect of preexisting LC_{20} phosphorylation on the magnitude of nocodazole-stimulated contraction, we used FBS to raise force and LC_{20} phosphorylation levels prior to addition of nocodazole. Cells precontracted with FBS showed a decreased contractile response to microtubule disruption. This result is inconsistent with the predictions of the tensegrity model but is consistent with microtubule disruption mediating contraction through an increase in LC_{20} phosphorylation. Furthermore, we found that nocodazole stimulated no further increase in LC_{20} phosphorylation of FBS-contracted cells, confirming that a component of the pathway leading to LC_{20} phosphorylation, utilized by both nocodazole and FBS, is saturated after FBS stimulation.

The similar increases in LC_{20} phosphorylation after treatment with 30% FBS for 80 min or 10 μM nocodazole for 30 min (Fig. 8) were unexpected because 30% FBS stimulates a 2- to 3-fold larger force increase than nocodazole. Also surprising was that the small additional contractile response to microtubule disruption in FBS-contracted cells was not associated with a measurable increase in LC_{20} phosphorylation. The interpretation of these differences between the changes in force relative to LC_{20} phosphorylation in FBS and nocodazole-stimulated contractions is complicated because the force and phosphorylation measurements were conducted on different preparations (FPCL vs. monolayer) and because of the possibility of a transient component to the LC_{20} phosphorylation increase following FBS stimulation (24). However, these apparent differences between the dynamics of LC_{20} phosphorylation and force suggest that LC_{20} phosphorylation may not be the only mechanism mediating the FBS- and nocodazole-stimulated contractions.

Microtubule Dynamics Are Coupled to LC_{20} Phosphorylation. The central finding of this work is the coupling of microtubule dynamics to LC_{20} phosphorylation. Although the physiological significance of this link between microtubule and microfilament dynamics is unknown, our findings are consistent with the hypothesis that microtubules organize motile functions of nonmuscle cells. In contrast to muscle cells, which are specialized for unaxial contraction, nonmuscle cells exhibit more complex motile activity. Cell locomotion and cell division involve contractions confined to specific regions of the cell (30, 31). Therefore, these functions are likely to utilize mechanisms that modulate myosin activity in specific regions of the cytoplasm.

Spatially inhomogeneous shifts in microtubule morphology or stability precede directed cell locomotion and cell division (31–34), suggesting that microtubules may direct the subcellular distribution of the forces driving these processes. The present results support a role for myosin activation, through LC_{20} phosphorylation, as a mechanism by which microtubules might direct the spatial pattern of contractility within cells.

Summary. Our purpose was to better define how microtubule disruption leads to cell contraction. Although our results do not rule out a contribution from a tensegrity mechanism, increased LC_{20} phosphorylation following microtubule disruption suggests that myosin activation may partially or fully explain the contractile and morphological effects of microtubule disruption. The interactions between microtubules and intracellular free Ca^{2+} regulation or other pathways leading to LC_{20} phosphorylation (28) remain an important question.

This work was supported in part by National Institutes of Health Grant GM38838. M.S.K. was supported in part by Medical Scientist Training Program Grant T32 GM07200.

1. Danowski, B. A. (1989) *J. Cell Sci.* **93,** 255–266.
2. Dennerll, T. J., Joshi, H. C., Steell, V. L., Buxbaum, R. E. & Heidemann, S. R. (1988) *J. Cell Biol.* **107,** 665–674.
3. Madreperla, S. A. & Adler, R. (1989) *Dev. Biol.* **131,** 149–160.
4. Tsutsui, H., Ishihara, K. & Cooper, G., IV (1993) *Science* **260,** 682–687.
5. Buxbaum, R. E. & Heidemann, S. R. (1988) *J. Theor. Biol.* **134,** 379–390.
6. Ingber, D. E. (1993) *J. Cell Sci.* **104,** 613–627.
7. Elson, E. L. (1988) *Annu. Rev. Biophys. Biophys. Chem.* **17,** 397–430.
8. Dugina, V. B., Svitkina, T. M., Vasiliev, J. M. & Gelfand, I. M. (1987) *Proc. Natl. Acad. Sci. USA* **84,** 4122–4125.
9. Arakawa, T. & Frieden, C. (1984) *J. Biol. Chem.* **259,** 11730–11734.
10. Ishikawa, R., Kagami, O., Hayashi, C. & Kohama, K. (1992) *Cell Motil. Cytoskeleton* **23,** 244–251.
11. Okuhara, K., Murofushi, H. & Sakai, H. (1989) *Cell Motil. Cytoskeleton* **12,** 71–77.
12. Sattilaro, R. F., Dentler, W. L. & LeCluyse, E. L. (1981) *J. Cell Biol.* **90,** 467–473.
13. Selden, S. C. & Pollard, T. D. (1983) *J. Biol. Chem.* **258,** 7064–7071.
14. Leiber, D. R., Jasper, J. R., Alousi, A. A., Martin, J., Bernstein, D. & Insel, P. A. (1993) *J. Biol. Chem.* **28,** 3833–3837.
15. Shinohara-Gotoh, Y., Nishida, E., Hoshi, M. & Sakai, H. (1991) *Exp. Cell Res.* **193,** 161–166.
16. Scott, C. W., Caputo, C. B. & Salama, A. I. (1989) *Biochem. J.* **263,** 207–214.
17. Serrano, L., Hernandez, M. A., Diaz, N. J. & Avila, J. (1989) *Exp. Cell Res.* **181,** 263–272.
18. Vallee, R. B., DiBartolomeis, M. J. & Theurkauf, W. E. (1981) *J. Cell Biol.* **90,** 568–576.
19. Kolodney, M. S. & Elson, E. L. (1993) *J. Biol. Chem.* **268,** 23850–23855.
20. Lamb, N. J., Fernandez, A., Conti, M. A., Adelstein, R., Glass, D. B., Welch, W. J. & Feramisco, J. R. (1988) *J. Cell Biol.* **106,** 1955–1971.
21. Broschat, K. O., Stidwell, R. P. & Burgess, D. R. (1983) *Cell* **35,** 561–571.
22. Cande, W. Z. & Ezzell, R. M. (1986) *Cell Motil. Cytoskeleton* **6,** 640–648.
23. Craig, R. (1983) *Nature (London)* **302,** 436–439.
24. Giuliano, K. A., Kolega, J., DeBiasio, R. L. & Taylor, D. L. (1992) *Mol. Biol. Cell.* **3,** 1037–1048.
25. Wysolmerski, R. B. & Lagunoff, D. (1990) *Proc. Natl. Acad. Sci. USA* **87,** 16–20.
26. Kolodney, M. S. & Wysolmerski, R. B. (1992) *J. Cell Biol.* **117,** 73–82.
27. Tomasek, J. J., Haaksma, C. J., Eddy, R. J. & Vaughan, M. B. (1992) *Anat. Rec.* **232,** 359–368.
28. Taylor, D. A. & Stull, J. T. (1988) *J. Biol. Chem.* **263,** 14456–14462.
29. De Brabander, M., Geuens, G., Nuydens, R., Willebrords, R. & De Mey, J. (1981) *Proc. Natl. Acad. Sci. USA* **78,** 5608–5612.
30. Jay, P. Y., Pham, P. A., Wong, S. A. & Elson, E. L. (1995) *J. Cell Sci.* **108,** 387–393.
31. Mabuchi, M. & Okuno, M. (1977) *J. Cell Biol.* **74,** 251–263.
32. Gundersen, G. G. & Bulinski, J. C. (1988) *Proc. Natl. Acad. Sci. USA* **85,** 5946–5950.
33. Rappaport, R. (1971) *Int. Rev. Cytol.* **31,** 169–213.
34. Rappaport, R. & Rappaport, B. N. (1974) *J. Exp. Zool.* **189,** 189–196.